Formation of IR emission in HII regions around young stars

Ya. Pavlyuchenkov, M. Kirsanova, V. Akimkin, D. Wiebe

Institute of Astronomy, Russian Academy of Sciences, Moscow, Russia

Abstract

We investigate the formation of IR emission and corresponding intensity distributions at 8, 24, and 100 micron in HII regions around young massive stars. The evolution of an HII region is simulated using an advanced chemo-dynamical model. Three dust components are included in the model: large silicate grains, very small graphite grains (VSG), and polycyclic aromatic hydrocarbon (PAH) particles. The emergent SED and intensity distributions are calculated using our RT model where stochastic heating of VSG and PAHs is taken into account. The efficiency of two processes for stochastic heating of VSG and PAHs is studied: the absorption of star emission and interaction with hot gas. We compare the synthetic maps with the observed maps from Spitzer and Herschel for the RCW 120 HII region. It is shown that the model with constant PAH abundance cannot reproduce the ring-like appearance of the observed intensity distribution at 8 micron. In order to explain the observed IR distributions we inspect two models of dust evolution. The first model assumes that PAHs are destroyed inside an HII region. In the second model the drift of the dust particles caused by radiation pressure is taken into account. We show that the model with PAH destruction is consistent with observed profiles given appropriate choice of the PAH destruction time. On the contrary, the model with the dust drift is not consistent with observations.

Introduction and goals of the study

One of the characteristic morphological features seen in infrared (IR) maps of the Galactic disk is so-called bubbles, that is, rings or fragments of rings in near-IR images (8–10 μm), mainly obtained in surveys performed with the Spitzer and WISE space telescopes. IR bubbles typically have different spatial distributions in the near and mid-IR. As a rule, the inner region of a bubble in Spitzer maps radiating at 24 μm is surrounded by a ring of 8-μm emission. Such intensity stratification seems to contradict to the expectation that inner regions must be hotter than outer regions. The origin of such inversed intensity distributions cannot be explained in simplified models and requires appropriate hydrodynamical, radiative transfer and dust evolution models.

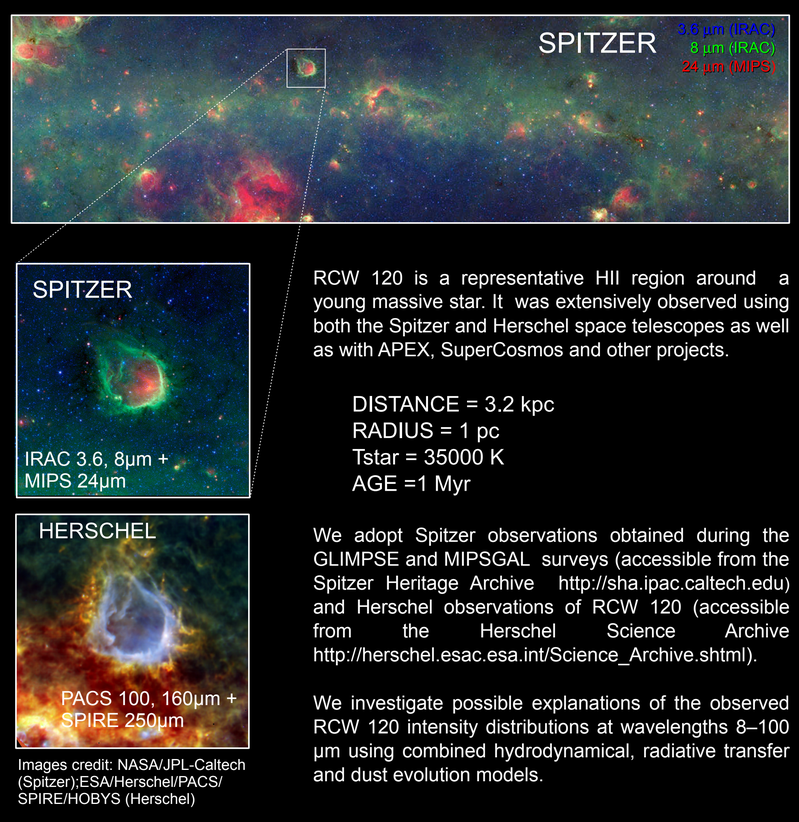

Images credit: NASA/JPL-Caltech (Spitzer);ESA/Herschel/PACS/ SPIRE/HOBYS (Herschel)

RCW 120 is a representative HII region around a young massive star. It was extensively observed using both the Spitzer and Herschel space telescopes as well as with APEX, SuperCosmos and other projects.

DISTANCE = 3.2 kpc
RADIUS = 1 pc
Tstar = 35000 K
AGE =1 Myr

We adopt Spitzer observations obtained during the GLIMPSE and MIPSGAL surveys (accessible from the Spitzer Heritage Archive http://sha.ipac.caltech.edu) and Herschel observations of RCW 120 (accessible from the Herschel Science Archive http://herschel.esac.esa.int/Science_Archive.shtml).

We investigate possible explanations of the observed RCW 120 intensity distributions at wavelengths 8–100 μm using combined hydrodynamical, radiative transfer and dust evolution models.

Model of an HII region

Gas dynamics

We use the chemo–dynamical model of an HII region by Kirsanova et al. 2009. This model traces the motion of ionization, dissociation, molecular evaporation from dust grains, and shock fronts during the expansion of the HII region into the surrounding molecular cloud. It also includes a chemical model, since this enables us to correctly calculate gas cooling and to treat the thermal balance in a self-consistent way at any moment in the evolution of the HII region.

Given uncertainties of exact physical conditions in RCW 120, we considered a number of dynamical models with different values of initial density and star temperature. The adopted distributions for a representative model are shown in Fig.1.

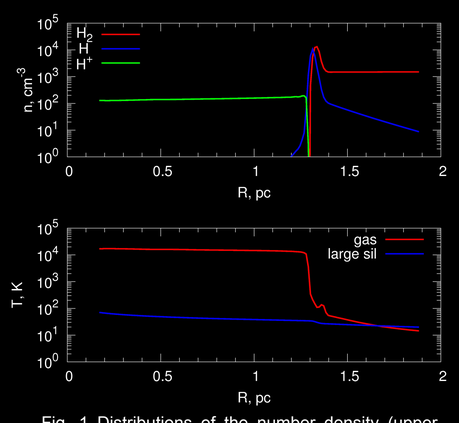

Fig. 1 Distributions of the number density (upper panel) and temperature (lower panel) for a model with initial density of 3000 cm^{-3}, star temperature of 35 000 K, and age of 170 kyr.

Radiative transfer

Since the mean thermal energy of a small grain and PAH particle in an HII region is comparable to the energy of a single UV photons, the temperature of such a grain fluctuates in time. This process is known as stochastic heating. In the general case, the thermal state of each dust type is described using the probability-density distribution over the temperature, P(T). The NATA(LY) software package described in Pavlyuchenkov et al. 2012 was used to compute P(T), SEDs and the radiation intensity distributions, presented in Fig.2-3.

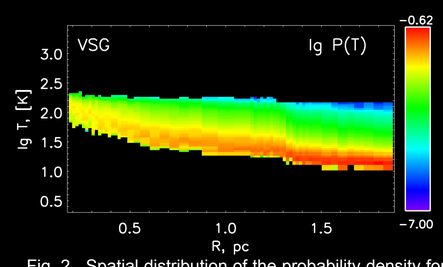

Fig. 2. Spatial distribution of the probability density for small graphite grains stochastically heated by stellar radiation.

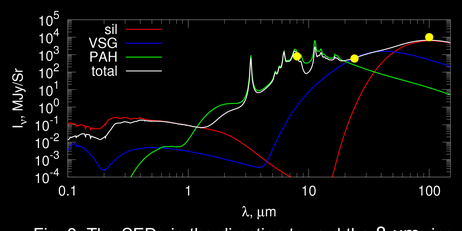

Fig. 3. The SEDs in the direction toward the 8 μm ring of the HII region. The spectra formed by the individual dust components and by all the components together are shown by different colors of curves. The yellow points show the observed intensities for RCW 120.

Dust evolution

We assumed that dust consists of three components: large silicate grains with radius of 3×10^{-5} cm, very small grains (VSGs) with radius of 3×10^{-7} cm, and polycyclic aromatic hydrocarbon (PAH) particles with radius of 7×10^{-8} cm. To describe dust density distributions the following three models were inspected:

Constant dust abundance. All dust grains do not evolve and are frozen to the gas. The dust-to-gas mass ratio is 0.01 while the relative abundances of VSGs and PAHs are chosen to provide quantitative agreement between the model and observations in terms of SEDs.

PAH evaporation. PAHs are destroyed by UV radiation. The evolution of relative PAH abundance x is given by: $dx/dt = G\cdot x/\tau$ where τ is the characteristic time for the PAH destruction in a standard UV radiation field and G is the intensity of the stellar radiation in units of the Draine interstellar radiation field. The spatial distributions of PAHs calculated for different values of τ are shown in Fig. 4.

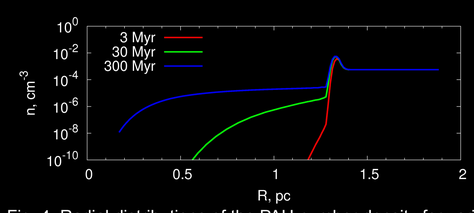

Fig. 4. Radial distributions of the PAH number density for various characteristic destruction times τ.

Dust drift. The dust grains are subject to radiation pressure and collisional friction with gas. Here we consider only direct collisions between gas and dust and do not take into account Coulomb collisions. In this approximation larger grains experience stronger drift. The obtained velocity distributions of dust grains are shown in Fig. 5.

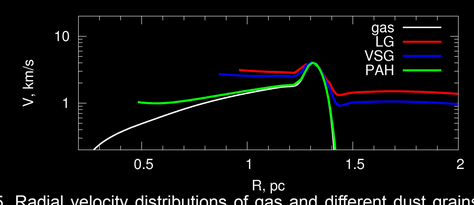

Fig. 5. Radial velocity distributions of gas and different dust grains in the model with the dust drift due to radiation pressure. Curves start at locations corresponding to the sweeping radii with zero dust density inside.

Results:

Constant dust abundance

While the model with well mixed dust does allow reproducing emission rings at all considered wavelengths, it definitely fails at 8 μm, predicting bright emission peak toward the region center that arises almost completely due to PAH emission. Emission at 24 μm has an alternating nature. Emission toward the ring is generated in comparable shares by PAHs and VSGs, while emission toward the center comes mostly from VSGs with some contributions from PAHs and hot large silicate grains. Note that at 100 μm our model predicts both ring-like emission and some emission toward the region center (that actually also comes from the dense shell around the HII region). This emission is not seen on Herschel maps. It remains to be seen whether this observed lack of emission is related to the source geometry or to the Herschel map building algorithm.

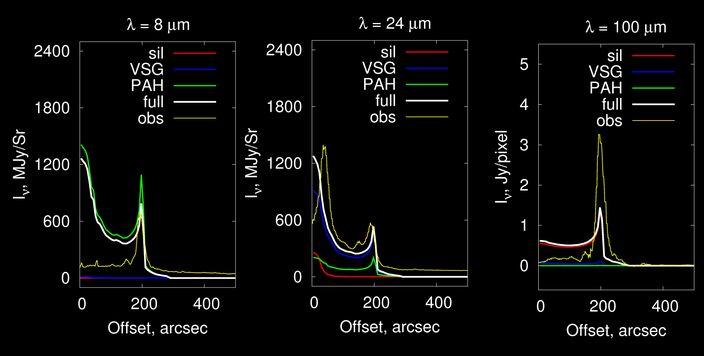

Fig. 6. Intensity distributions at 8 μm (left), 24 μm (middle), and 100 μm (right) for the model with constant dust abundance. The profiles formed by the individual dust components (sil – large silicate grains, VSG – very small grains, PAH – polycyclic aromatic hydrocarbons) and by all the components together (total) are indicated by different colors. The yellow curves (obs) show the observed profiles for RCW 120.

PAH evaporation

We have seen in Figure 6 that the model with constant dust abundance allows reproducing maps at longer wavelengths and fails at 8 μm where nearly all the emission comes from PAHs. Thus, it is enough to account for PAH destruction to remove the discrepancy. We have considered three representative destruction times, 3, 30, and 300 Myr for the standard Draine field (as *G* is of the order of 10^6 in the considered models, this translates to PAH lifetimes about few million years and less). Plots presented in Figure 7 show that even τ as long as 300 Myr decreases the central PAH emission well below the emission from the ring. To account for the observed 8 μm emission level, we need to assume that the characteristic PAH destruction time is about 30 Myr or less.

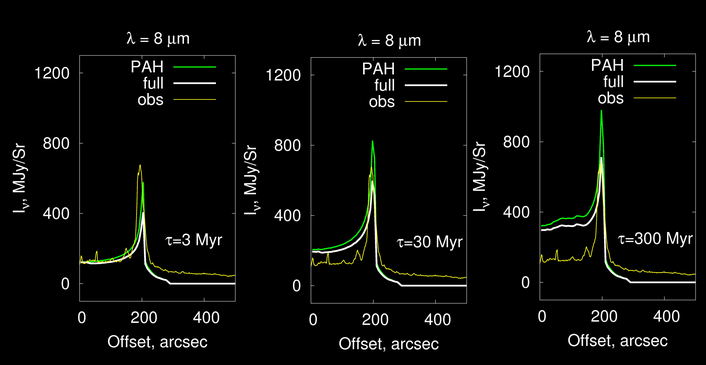

Fig. 7. The 8 μm intensity distribution for models with various characteristic PAH destruction times. The white curves (total) show the model profiles and the yellow curves (obs) show the observed profile for RCW 120. The green curves show the contribution of the PAH emission.

Dust drift

Photoevaporation is not the only way to remove dust from the star vicinity. Combined action of radiation pressure and gas drag also purges dust from the interior of the region affecting predominantly large grains. At 100 μm dust drift does solve somewhat the problem of the excess emission toward the RCW 120 center. As PAH particles are almost frozen to gas, radiation pressure is not nearly as effective in removing them from the HII region as photoevaporation. The central emission peak seen in Figure 6 disappears but the remaining emission is still way too bright in comparison with observations. The most serious discrepancy arises at 24 μm. An emission peak (or a compact ring), observed at this wavelength, disappears almost completely in the model with dust drift. Thus, we conclude that dust drift alone is not a viable mechanism to explain the observed IR map morphology in HII regions.

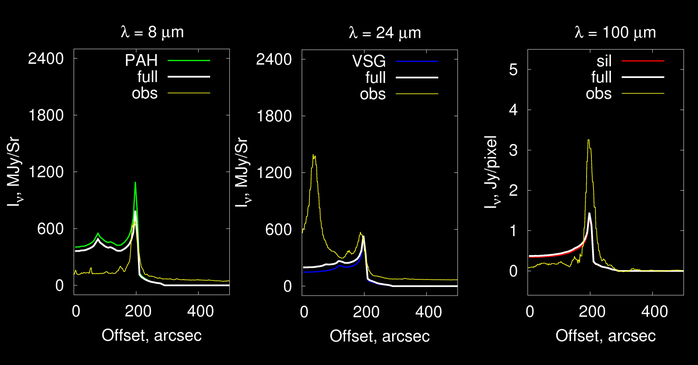

Fig. 8. The intensity distribution for the model with dust drift due to radiation pressure. The white curves (total) show the model profiles, the yellow curves (obs) show the observed profiles for RCW 120, the curves with other colors show the main contributions from various dust types.

References

Pavlyuchenkov et al., Astron. Rep. 57, 573 (2013)
Kirsanova et al., Astron. Rep. 53, 611 (2009)
Pavlyuchenkov et al., MNRAS 421, 2430 (2012)